Research Article

Enhanced cell viability and cell adhesion using low conductivity medium for negative dielectrophoretic cell patterning

Srinivasu Valagerahally Puttaswamy[1], Shilpa Sivashankar[1], Rong-Jhe Chen[1], Chung-Kuang Chin[1], Hwan-You Chang[2] and Cheng Hsien Liu[1]

[1] Department of Power Mechanical Engineering, National Tsing Hua University, Hsin Chu, Taiwan
[2] Institute of Molecular Medicine, National Tsing Hua University, Hsin Chu, Taiwan

Negative dielectrophoretic (n-DEP) cell manipulation is an efficient way to pattern human liver cells on micro-electrode arrays. Maintaining cell viability is an important objective for this approach. This study investigates the effect of low conductivity medium and the optimally designed microchip on cell viability and cell adhesion. To explore the influence of conductivity on cell viability and cell adhesion, we have used earlier reported dielectrophoresis (DEP) buffer with a conductivity of 10.2 mS/m and three formulated media with conductivity of 9.02 (M1), 8.14 (M2), 9.55 (M3) mS/m. The earlier reported isotonic sucrose/dextrose buffer (DEP buffer) used for DEP manipulation has the drawback of poor cell adhesion and cell viability. A microchip prototype with well-defined positioning of titanium electrode arrays was designed and fabricated on a glass substrate. The gap between the radial electrodes was accurately determined to achieve good cell patterning performance. Parameters such as dimension of positioning electrode, amplitude, and frequency of voltage signal were investigated to optimize the performance of the microchip.

Received 6 June 2010
Revised 17 August 2010
Accepted 27 August 2010

Keywords: Cell adhesion · Cell patterning · Medium conductivity · Negative dielectrophoresis · Osmolarity

1 Introduction

In the recent years, there has been tremendous progress in the research of manipulation and analysis of biological cells at the microscale. The enhanced interest is the reason for applying micro electro mechanical systems for selective trapping, manipulation and separation of micro/nano bio-objects. The bio-objects with the size ranging from 10 nm to 100 μm can be manipulated by exploiting the use of electrical force as it dominates at the microscale. The methods used in practice are electrophoresis, electroosmosis, electrowetting, electrofusion and dielectrophoresis (DEP).

Herbert Pohl was the first to coin the term "dielectrophoresis" in 1951 [1]. He defined this as "the motion of suspensoid particles relative to that of the solvent resulting from polarization forces produced by an inhomogeneous electric field". It is used in a wide range of applications [2], such as separation and isolation of cells [3, 4], cell handling prior to electro fusion [5] and cell sorting [6]. Under a non-uniform electric field, DEP results in the movement of cells. When a particle is more polarizable than the immersion medium, the resulting force will direct the particle towards the regions of electric field maxima. This phenomenon is known as positive DEP (p-DEP). Negative DEP (n-DEP) occurs when the cell is less polarizable than the suspending medium in a non-uniform electric field, and describes the movement of particles away from high field regions. When cells are subjected to a DEP force, cell damage occur mainly for three

Correspondence: Dr. Cheng Hsien Liu, Microsystems and Control Laboratory, Department of Power Mechanical Engineering, National Tsing Hua University, Hsinchu, Taiwan 300, ROC
E-mail: liuch@pme.nthu.edu.tw

Abbreviations: DEP, dielectrophoresis; **FDA/EtBr**, fluorescein diacetate/ethidium bromide; **n-DEP**, negative DEP; **p-DEP**, positive DEP

reasons: (i) there may be excessive charging of the cell membrane exposed to electric field [7–9], (ii) the cells are suspended in a non-physiological medium, and (iii) shear stress is induced due to fluid flow. When the flow rate is low, the induced shear stress is negligible. On the other hand, the first two reasons are important for the cell viability and cell adhesion.

Several studies have focused on the use of high conductivity medium for n-DEP manipulation of living cells. However, it requires complicated and extreme miniaturization of electrodes at high-frequency electric field (between 10 MHz and several hundred MHz with the field strength of 50–100 kV/m) [10, 11]. Exposing biological cells to such a high electric field environment might lead to a variety of profound biochemical and biophysical effects, such as apoptosis and cell lysis [12]. Many investigations [13–15] have revealed that the effects of Joule heating can result in low efficiency of column separation, reduction of analysis resolution, and even loss of introduced samples. Joule heating may create a temperature gradient, and can also cause an increase in temperature [16]. One of the side effects of DEP is therefore temperature increase in the high conductivity medium in which the cells are suspended, disturbing the favorable cellular environment. In our group, we have used low conductivity DEP buffer for liver cell patterning using p-DEP to mimic liver lobule [17]. In contrast, the DEP buffer, although excellent for DEP manipulation, is unsuitable for studying cell adhesion and cell growth. In addition, the voltage and frequency required are still high, and will reduce the cell viability and adhesion rate drastically. *e.g.*, during the 1 h of manipulation in the earlier reported DEP buffer.

Efficient DEP cell manipulation requires a low conductivity buffer. In addition, low conductivity DEP buffer also reduces certain undesired effects caused by a regular biological buffer like phosphate-buffered saline (PBS) during DEP operation [18].To overcome the above limitations, we have developed a low conductivity medium that has the components of native culture medium, *i.e.*, Dulbecco's modified Eagle medium (DMEM), at low concentration suitable for DEP-based cell manipulation at low voltage and frequency with high percentage of viability and cell adhesion. The dimension of the electrodes was optimized to provide a well defined non-uniform electric field, and thus generate n-DEP forces. This proposed n-DEP method can also be used to achieve cell patterning and minimize hazardous effect on living cells. The n-DEP phenomenon is preferable to p-DEP for cell patterning, because the cells are trapped away from high field regions and are less likely to experience large transmembrane potentials that could develop.

2 Materials and methods

2.1 Materials

Calcium chloride (anhydrous), ferric nitrate, potassium chlorate, magnesium sulfate (anhydrous), sodium chloride, sodium bicarbonate, sodium hypophosphate, D-glucose, sodium pyruvate, vitamins and amino acids were purchased from Sigma-Aldrich. The 12800 DMEM medium and fetal bovine serums (FBS) were obtained from Sigma and Biological Industries, Israel, respectively. Altered media (M1, M2 and M3) were used for all the experiments and conventional medium DMEM was used to culture the cells. All reagents were of analytical grade and ultrapure water (resistance 18.36 Mohm/cm) produced by Millipore Milli-Q system was used throughout.

2.2 Design, fabrication and working principle of cell patterning on microchip

The liver is considered as a difficult object to reconstruct due to its complex cellular architecture. Structurally, the liver is morphologically divided into lobules that take the shape of irregular polygonal prisms. The lobule is filled with cords of liver parenchyma cells, hepatocytes, which radiate from the central vein and are separated by sinusoid-like vascular endothelial lining cells. In a 3-D morphology, the liver tissue is more like regularly branching and interconnecting sheets, which extend in parallel to the long axis of the lobule and radiate out from the center, as illustrated by our group earlier [17]. In our design, by constructing the geometric shape and the distribution of radial DEP electrodes, the desired spatial electric-field gradients are enhanced to guide and snare individual cells to form the desired lobule-mimetic pattern. The array electrodes provide inhomogeneous electric field gradients to manipulate cells via field-induced DEP, as shown in Fig. 1A, with the simulation of electric field distribution. The electrodes are arranged in parallel to radiate out from the center.

With this proposed microfluidic chip design, the original randomly distributed hepatocytes inside the microfluidic chamber can be manipulated in parallel and align into the desired pearl-chain array pattern. This radial pattern mimics the lobular morphology of real liver tissue. A commercial finite element software CFD-ACE+ (CFDRC, Huntsville,

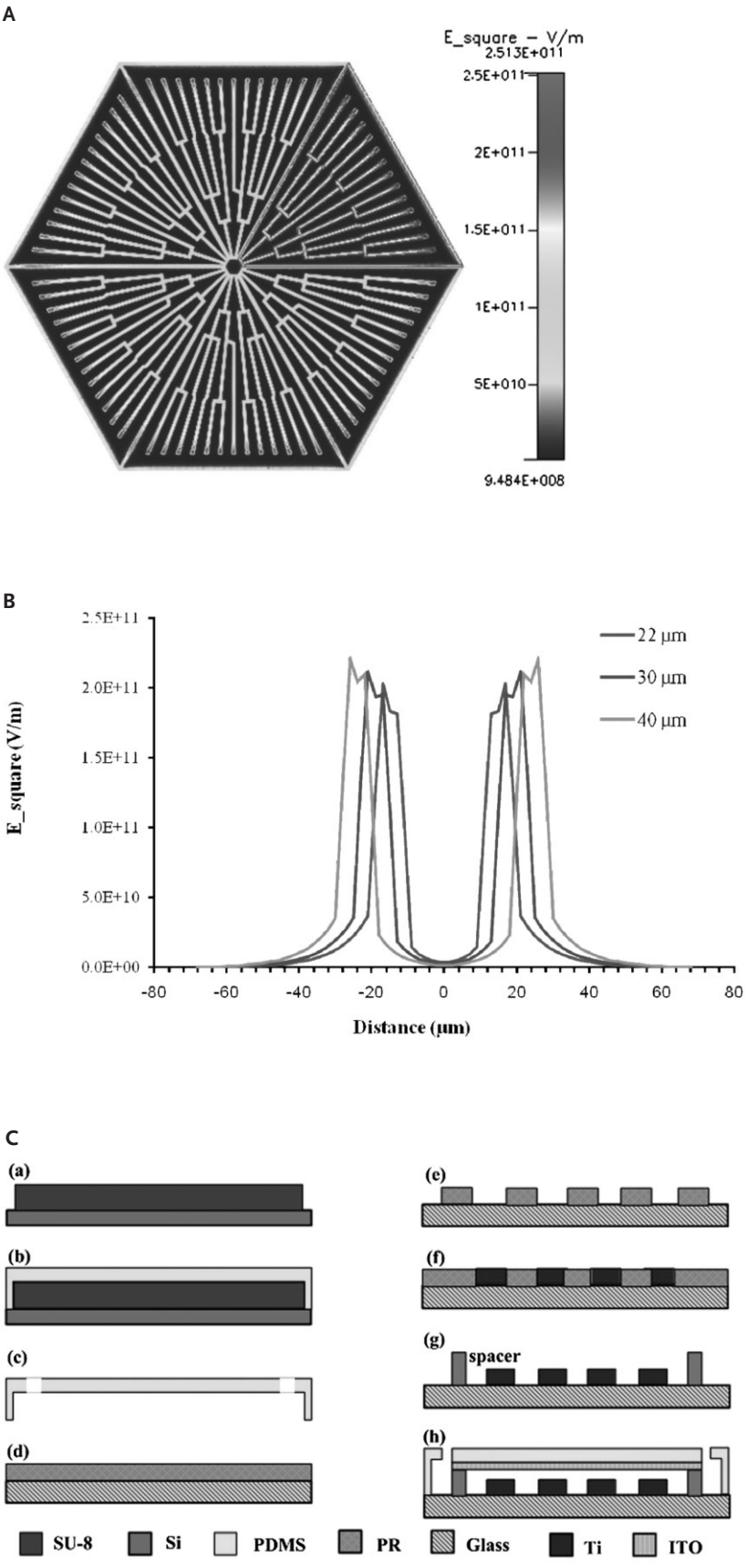

Figure 1. CFD-ACE+ simulation results. (A) The electrode design with the distribution of root mean square AC electric field [E square (v/m)]. (B) Width of stable region between electrodes for varying distance between a pair of electrodes. This is an important criterion during n-DEP for alignment of the cells in the stable region. (C) Microfabrication process for cell patterning on chip: (a) SU-8 negative photoresist is used to define microchannels and pattering chamber (100 μm in height). (b) PDMS is micromolded to serve as the transparent top cover. (c) The fluidic connections are mechanically punched through on the PDMS top cover. Microfabrication process for titanium electrodes on glass substrate. (d) Photoresist (PR) was spin coated onto a glass substrate. (e) Photoresist was exposed to UV rays through a mask to obtain patterned photoresist structures after developing. (f) Titanium deposited by E-Gun Evaporation. (g) Fine patterned titanium electrodes obtained by lift-off process and spacers were attached to provide space for microfluidic flow.(h) ITO glass was placed on the spacers and PDMS was bonded to the substrate via plasma bonding.

Biotechnol. J. 2010, 5, 1005–1015

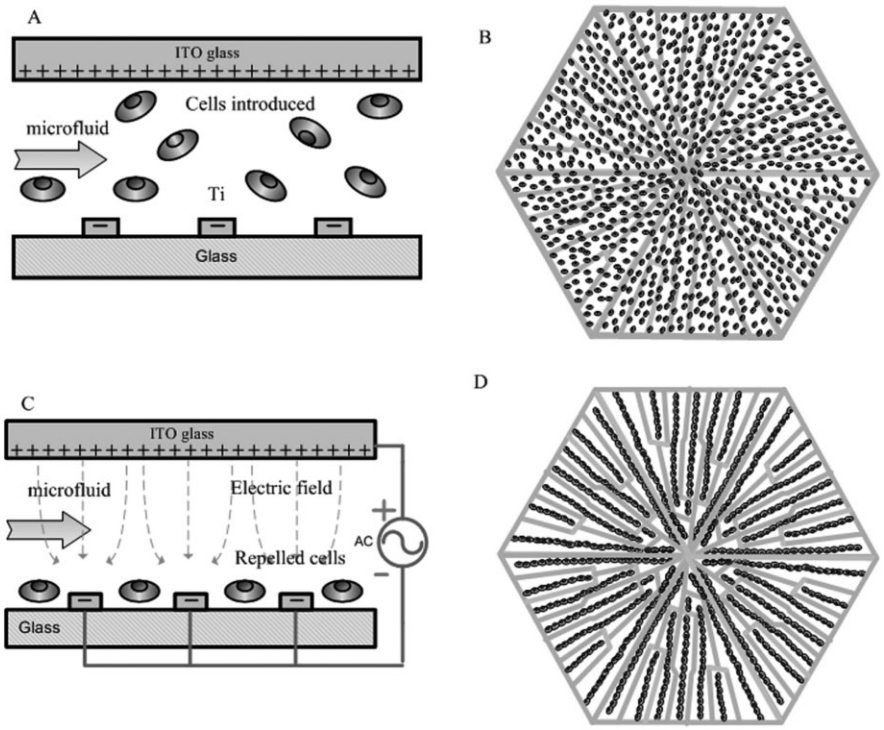

Figure 2. Working principle of liver-cell patterning chip. (A, B) Side and top schematic view of the spatially randomly distributed cells. (C, D) Side and top schematic view of the cell patterning by n-DEP effect.

AL) was used to simulate the induced electric field. The CFD-ACE+ simulation results showed the electric field distribution across two adjacent radial electrodes [19]. The gaps between the radial electrodes were determined to produce a good cell-patterning performance. The width of the electrode was set at 8 μm as it provided high electric field strength near the surface electrodes, with the gap varying from 22 to 40 μm as shown in Fig. 1B.

The microfabrication process of the cell patterning chip is summarized and illustrated in Fig. 1C. To fabricate a polydimethylsiloxane (PDMS) microfluidic channel, a silicon substrate was prepared using the piranha clean technique. The chamber and microchannel height of 100 μm was defined using SU-8 negative photoresist. PDMS prepolymer was mixed with a curing agent at a 10:1 mass ratio and degassed in a vacuum chamber to remove the air bubbles. Silicon tubes were placed accurately at the inlet and outlet position on the silicon-PR master mold and PDMS poured carefully. After degassing in a vacuum chamber again, PDMS was cured by heating in an oven. The PDMS layer was peeled off from the master mold. To form a complete microfluidic device, the peeled PDMS layer was permanently bonded to the glass by applying O_2 plasma in O_2 plasma equipment. This plasma treatment also makes the walls of the microchannel hydrophilic, which is favorable for introducing the sample into the device. The complete device was connected to the external fluidic system via silicone tubes.

A chip with titanium electrodes were designed and fabricated on a glass substrate using a photolithography process that has been widely used for making the microchips. In this technique; electrodes were generated using light-sensitive photoresist AZ5214 and chrome on a glass mask. At first, the photoresist was spin coated onto a clean glass substrate and exposed to ultraviolet (UV) light through a customized mask containing the desired opaque pattern aligned by EV620 mask aligner. The exposed part of the photoresist was solubilized in a developer solution, resulting in a photoresist pattern. Electrodes were micromachined on a glass substrate using the photolithography process with the E-Gun evaporation of a 200-Å titanium layer. Finally, the fine titanium electrodes were obtained using a lift-off process.

Figures 2A–D illustrate the working principle of liver cell patterning chip. The liver cells were injected into the microfluidic chamber with a continuous flow input, guided along the stream and randomly distributed, as illustrated in Figs. 2A and B. The cells flowed into the cell patterning area above the radial electrodes. When an adequate alternating current (AC) potential was applied, the cells were manipulated by the balance force contributed

by the field-induced DEP and the hydrodynamic force. The randomly distributed cells were repelled by n-DEP effect to form a pearl chain between the electrodes, as illustrated in Figs. 2C and D.

2.3 Preparation of new medium for DEP

Media with different conductivity, osmolarity and pH were prepared mainly by varying the salt concentration. The basic culture medium DMEM has high conductivity (1856 mS/m) due to its high salt concentration and is not suitable for the DEP operation. Medium M1 contains 99.18 g/L sucrose, 2.38 g/L HEPES and 0.5% DMEM [20]. M2 comprises sucrose and dextrose, and, compared to DMEM, a decreased $CaCl_2$ (10%) and NaCl (1%) concentration. M3 consists of 90 g/L sucrose and 2.25 g/L dextrose with only 1.5% of the NaCl component of DMEM and 6% of $CaCl_2$. In M2 and M3 all the components of the basic culture medium are present but in reduced quantity. The compositions of the media are summarized in Table 1.

2.4 Measurement of conductivity, osmolarity and pH of the media

The conductivity of the media was calibrated using a conductivity meter Cond 330i (WTW GmbH, Germany, 0.5% accuracy). Osmolarity was measured using an Advanced Micro Osmometer 3300 (Advanced Instruments, Inc., Laboratory Products Division, Norwood, MA, USA). The pH was measured using a pH meter (Eutech Instruments Cyberscan PH 1500 Phion Meter). All readings were taken at 25°C. The average value of all the readings was determined from at least three measurements.

2.5 Cell manipulation experiments

2.5.1 Cell culture

Human liver cell line HepG2 (ATCC, HB8065) was maintained at 37°C with 95%/5% air/CO_2 in DMEM, containing 10% heat-inactivated FBS and antibiotics (100 U/mL penicillin and 100 U/mL streptomycin; Sigma-Aldrich). Replicate cultures were obtained by trypsinization and were used for up to five passages [21]. The human liver cell line identification was confirmed by their polygonal morphology.

2.5.2 Cell preparation for DEP manipulation

Prior to the on-chip cell patterning demonstration, HepG2 cells were harvested from subconfluent cultures, detached using 0.2% trypsin (Sigma) with 1 mM EDTA (Sigma) in PBS and re-suspended in the three media and the DEP buffer, one at a time, to give a final concentration of 5×10^6 cells/mL. In cell patterning demonstrations and experiments, HepG2 cells were pre-labeled with biocompatible fluorescent dyes DiO (green, excitation/emission wavelengths of 549/565 nm) according to manufacturer's protocols (Molecular Probes, Eugene, OR, USA), and identified using a fluorescent microscope (BX-51, Olympus, Tokyo, Japan). Cells were immediately used for DEP-based cell manipulation and patterning experiments.

2.5.3 Experimental set up for DEP-based cell patterning

A syringe pump (SP230IW, WPI, Florida, USA) was used to pump and regulate the flow of the fluid. To generate the out-of-phase AC voltage for the DEP operation on the microchip, a function generator

Table 1. Composition of the modified medium used for DEP manipulation and the further tests along with native culture medium[a)]

Components	DMEM (mg/L)	DEP buffer (mg/L)	M1 (mg/L)	M2 (mg/L)	M3 (mg/L)
HEPES	–	2385	2380	–	–
Sucrose	–	80700	99180	90000	90000
Dextrose		4500	10600	2250	2250
Amino acids	100 % as per catalog	–	0.5 % of DMEM	15 % of DMEM	10 % of DMEM
Vitamins	100 % as per catalog	–	0.5% of DMEM	15% of DMEM	10% of DMEM
Salts					
$CaCl_2$	200	11.1	1	20	12
$Fe(NO_3)_3 \cdot 9H_2O$	0.1	–	0.0005	0.001	0.0015
KCl	400	–	2	4	6
$MgSO_4$ (anhyd.)	97.67	–	0.488	0.98	1.47
NaCl	6400	–	32	64	96
NaH_2PO_4	125	–	0.625	1.25	1.88
Sodium pyruvate	110	–	0.55	1.1	1.65

a) More detailed information about composition of DMEM (12800) can be found in INVITROGEN cell culture catalog 2008/2009.

(33120A, Agilent) was employed. Electrical input signals were checked using an oscilloscope (54624A, Agilent). An inverted microscope (BX-51, Olympus, Tokyo, Japan) was used to keep track of the motions and displacements of cells. Movies and images were captured and recorded via a digital CCD camera connected to a computer.

2.5.4 Cell viability assay

The cell viability was assessed with the fluorescein diacetate/ ethidium bromide (FDA/EtBr) (Sigma) viability/cytotoxicity assay, which could distinguish the live cells from the dead cells via the FDA/EtBr dyes [22].The viability assays were done on microchips during manipulation with the altered media and DEP buffer. The live cells are green and the dead cells are red in color. FDA dyes are highly lipophilic and readily pass through the plasma membranes of the cells. Its acetyl ester groups are then cleaved by intracellular esterase activity to generate fluorescein. EtBr passes through the porous membranes of the dead cells and binds to nuclear DNA, which stains dead cell nuclei red. The cell viability was measured using ImageJ software (National Institute of Health, USA) by measuring cell population.

2.5.5 Cell adhesion assay

Cells were suspended in medium (M1, M2, M3 or DEP buffer) for 20, 50, 80, 110, or 140 min and incubated in Eppendorf tubes. After the allocated time, the cells were centrifuged, re-suspended in a 60-mm culture dish containing conventional DMEM and cultured for 12 h. The cells were stained with FDA/EtBr dye and the morphology of cells was observed through a fluorescent microscope [23]. ImageJ software (National Institute of Health, USA) was used to measure adhered cell population.

3 Results and discussion

3.1 Conductivity, osmolarity and pH of the media used

Table 2 tabulates the measured values of all the parameters mentioned above. The conductivity of M1, M2 and M3 was reduced below that of the DEP buffer, which is well suited for DEP manipulation [17]. The osmolarity values were within physiological values obtained for DMEM (300–340 mOsm/kg) [24]. The measured values of pH for the media were also well within the physiological values (7.0–7.4) with the exception of medium M1, which was 4.5. The pH and osmolarity of the prepared media were close to the values of the native cell culture medium (DMEM), which helped to minimize the influence on cell functioning.

Table 2. Measured values for specific pH, conductivity, and osmolarity of media[a)]

Parameters at 25°C	DMEM	DEP buffer	M1	M2	M3
pH	7.2	6.8	4.5	7.1	7.21
Conductivity (mS/m)	1856	10.2	9.02	8.14	9.55
Osmolarity (mOsm/kg)	338	356	348	330	304

a) All the values of the media M2, M3, buffer and DMEM are well within the physiological values. The pH of M1 is acidic.

To ensure long-term cell viability and minimize environmental stress on cells, it is beneficial to keep the cells suspended in their native culture medium (DMEM). This medium is composed of the required nutrients and is also osmotically balanced [25]. In contrast, the high electrical conductivity of such media restricts the use of DEP manipulation techniques because it may result in a heating effect and generate electrolytic bubbles during DEP, causing damage to the cells [17]. Therefore, we developed new media with varying concentrations of the native culture medium components. Our preferred method of conductivity reduction was desalting. To formulate these media, sucrose was added to maintain the osmolarity and physiological condition. HEPES was added in medium M1 to act as the buffering agent. In media M2 and M3, compared to M1, $CaCl_2$ was increased to 10% and 6%, respectively, whereas HEPES was not added to maintain optimal pH value. Ca^{2+} plays an important role in cell growth, cell adhesion and the regulation of many cell functions. The Ca^{2+} signal in cells for hormonal stimulation is partly transmitted to the intracellular responses, which are mediated through a family of Ca^{2+}-binding protein [26–28]. Salt components, amino acids and vitamins were added to favor the cell viability during and after DEP manipulation of the cells.

3.2 Manifestation of n-DEP-based cell patterning

To demonstrate the cell patterning for human liver cells, HepG2 of about 10–15 μm in diameter were used. Human liver cells are more delicate than some other cells and bacteria. It is easier to observe the cell damage and the medium harm due to DEP manipulation using these cells. The cells were introduced into the microchip with the media (5×10^6 cells/mL) from the inlet via a syringe pump with a flow rate of 5–25 μL/min. The DEP voltage was turned on for parallel cell manipulation once flow was steady and the cells were evenly distrib-

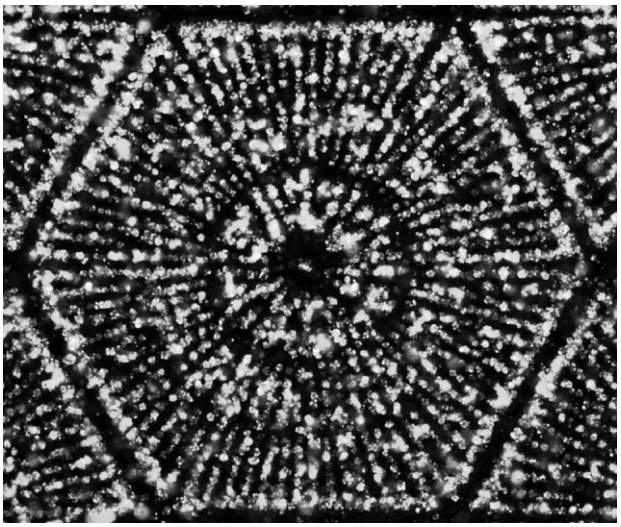

Figure 3. On chip demonstration of n-DEP cell patterning. HepG2 cells were pre-labeled with fluorescent dye DiO (green). The randomly distributed cells are bee lined between the radial electrodes and proximate the radial cell pattern of a typical liver lobule.

uted in the cell patterning chamber. The randomly distributed cells were bee-lined between the radial electrodes, which proximates radial cell pattern of typical liver lobule as represented in Fig. 3.

Our cell patterning demonstrations were performed in n-DEP modes in all the media (M1, M2, M3 and DEP buffer). Based on our early research [17], the cells were manipulated using p-DEP mode at the 5 V peak-peak at 1 MHz in the DEP buffer. In contrast, as shown in Table 3, n-DEP phenomena can be clearly observed at the 2 V peak-peak at 850 Hz in the newly prepared medium M2. The voltage and the frequency required for the n-DEP phenomenon is less than that required for DEP buffer and the conventional DMEM without any limitation to either the diminutive electrode size or the advanced fabrication technology. Both the voltage and the frequency required to exhibit n-DEP phenomena in M1and M3 were also lower (Table 3). It was also evident that the electric current was reduced with the use of low conductive media, which in turn decreased the heating of cell suspension. In addition, less power is required for the electropulsator because of lower electric current [29]. The reduction in salt components in the media resulted in low ion concentration, thereby reducing both the voltage and the frequency required for the DEP manipulation.

Table 3. Voltage, current and frequency required to exhibit n-DEP phenomena

	n-DEP		
Media	**Voltage (V)**	**Current (μA)**	**Frequency (Hz)**
DEP buffer	5	25	1000
M1	3	18	900
M2	2	15	850
M3	3	20	950

3.3 Effects of the DEP manipulation on cell viability

In the earlier reported DEP buffer, cell viability and adhesion rate drastically decreased during the 1 h of manipulation. In the present work, the low conductive medium was used to enhance cell adhesion and cell viability during DEP-based cell patterning to mimic liver lobule. Therefore, the cell viability was evaluated as patterned. For all DEP-based cell manipulation experiments, the cells must be suspended in the DEP buffer from loading, patterning, to attachment. This manipulation period typically lasts for 30–60 min. After that, the DEP buffer is replaced with optimal growth medium. However, all DEP buffers described in the published literatures cause severe damages to cells, even as robust as hepatoma cells, when used for longer period (more than 30 min). This problem significantly limits the use of DEP to manipulate cells. The proposed low conductive medium can maintain the trait of the cells for a longer period during and after DEP manipulation. The improvement of cell viability to 2–3 h using our low conductivity medium will allow the use of most, if not all, DEP systems applicable to cell study.

Once the liver cells were patterned, FDA/EtBr dyes were introduced into the cell patterning chamber from the inlet for 30, 60 and 90 min. The cell viability test results using the FDA/EtBr fluorescence assay are shown in Figs. 4A–L at the 5 Vpeak-peak in the three different media and DEP buffer. The fluorescence microscope image of on-chip patterned liver cells simultaneously represents both the viable cells (stained with green fluorescence) and the dead cells (stained with red fluorescence). The viability of cells varies according to the time in individual medium.

Further, we exposed and held the DEP manipulated cells in the DEP buffer and the altered media with several AC electric-field excitations. Experimental results indicated that the cell viability in the trials over 30 min was about 50 ± 3.4% in DEP buffer, 62 ± 2.4% in M1, 95 ± 1.5% in M2 and 88 ± 3.2% in M3. In addition, on maintaining the patterned cells over 60 min, cell viability was about 8.5 ± 1.1% in the DEP buffer, 40 ± 1.4% in M1, 90 ± 1.2% in M2, and 78 ± 2.2% in M3. The cell viability further deteriorated to 1.3 ± 1% in DEP buffer and 10±1.5% in medium M1 whereas, the viability was appreciably

Biotechnol. J. 2010, 5, 1005–1015

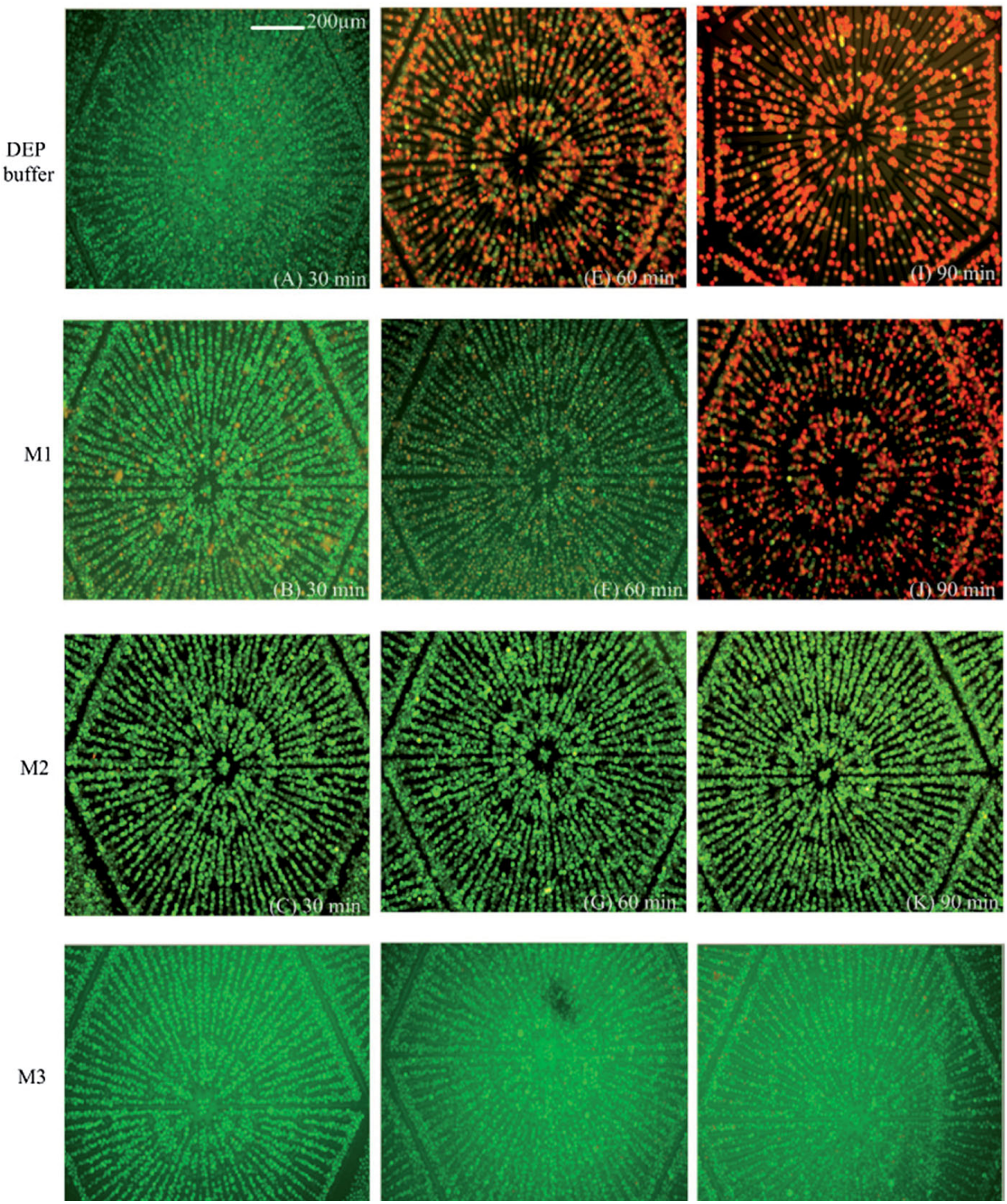

Figure 4. Assessment of HepG2 viability in DEP buffer and different media with AC electric field treatment. (A–L) Fluorescence microscopy images from the *in situ* FDA/EtBr cell viability assay. HepG2 cells were patterned during n-DEP manipulation at a 1 kHz AC potential of 5 V peak-peak (A, E, I) for DEP buffer, 1 kHz AC potential of 5 V peak-peak (B, E, J) for medium M1, 900 Hz AC potential 5 V peak-peak (C, G, K) for medium M2, 900 Hz AC potential at 5 V peak-peak (D, H, L) for medium M3. Viable cells fluoresce green and dead cells fluoresce red. The DEP operation was carried out for three different time periods: 30, 60, and 90 min and the results are shown. All data represent mean ± SD (n=3). * p<0.05, ** p<0.01, and *** p<0.001 versus control (control: viability in earlier reported DEP buffer). The entire picture is shown in n-DEP mode.

maintained at 82% ± 2.3% and 69% ± 1.8% in M2 and M3, respectively, for 90-min exposure.

The cell viability rate drops quickly and even drastically for human liver cells in the DEP buffer, which confirms to the results of Ho *et al*. on *Lab on Chip* [17]. The viability decreased in medium M1 because of the acidic nature of medium. Addition of HEPES to medium M1 resulted in a drastic reduction of pH value to acidic values. This acidic medium causes cell death, and these dead cells themselves turn into acids. If some cells survive, they become abnormal. The increased viability in medium M2 and M3 was due to the increased percentage (compared to M1) of $CaCl_2$, remaining salt components, amino acids and vitamins. Both pH and osmolarity values were well within the physiological value. Our experimental results prove that cell survival in experiments involving electropermeabilization can be improved by decreasing the medium conductivity [28].

Viability of cells increased with a decrease in applied voltage and frequency required to manipulate the cells, as depicted in graph presented in Figs. 5A–C. Another environmental stress on the DEP manipulated cells came from the external AC electric field excitation. The voltage required for the execution of DEP manipulation plays an important role in the cell viability rate. Synonymously, frequency was also a critical parameter in the monitoring the viability of cells.

From Table 3, it is evident that the voltage and frequency required for the n-DEP manipulation of human liver cells are significantly less for M1 and M2 than those required for DEP buffer. A similar trend can also be seen with medium M3. The reduced voltage and frequency are the importunate reasons for the enhancement of cell viability [5].

3.4 Effects of the media on cell adhesion

Most cells, except those of blood origin, must adhere onto a solid surface to survive. The adhesion ability of cells is a valuable indicator of cell viability and functionality. Various hydrodynamic techniques and methods have been developed to generate high shear stress and detach strongly adhered cells; these include the spinning disk apparatus [30], radial flow chambers [31] and rectangular parallel plate flow chambers [32]. Recently adhesion strength of single cells has been analyzed by Christ *et al*. [33], and microfluidic shear devices have been utilized for quantitative analysis of cell adhesion [34]. The flow/shear approach to cell adhesion assay mentioned in the earlier studies [30–34] is commonly used to measure the cell-substratum interaction force, which is cell-type dependent and can be used to explain different behaviors of cells. On the other hand, in the present study the flow rate was minimal so that the cells were not subjected to high flow rate and high shear stress. The adhesion assay used in this study (FDA/EtBr cell adhesion assay) is considered as a general cell viability indicator because dead cells are incapable of adhering on the device surface [35].

During the cell adhesion assay, the cells were cultured for half a day after suspension in the media, and then stained with FDA/EtBr dyes; the cell morphology was observed using a fluorescent microscope. The adhered cells with intact morphology fluoresced green, whereas the dead cells fluoresced red. Within 20 min, about 90 ± 2.5%, 95 ± 1.5% and 92 ± 2.2% of the HepG2 cells grew well and adhered to the substrate when exposed to the DEP buffer, medium M2 and M3, respectively. Cell adhesion remained the same for media M2 and M3, whereas it declined steeply over 30–50 min when suspended in DEP buffer, and few cells survived after this time period. Meanwhile, about 85% of cells adhered to the substrate even after 120 min of suspension in media M2 and M3. The experimental data of the cell adhesion ability are presented in Fig. 6.

Although the cell adhesion rate in the DEP buffer was good for the first 20 min of suspension, it drastically decreased with time and only a countable number of cells adhered to the substrate after 60 min of suspension. In medium M1, the cell adhesion was very poor in the first 20 min due to the acidic nature of the medium. The adhesion rate of cells in M2 and M3 was significantly better even after 120 min of suspension, which meant that the cells could withstand such environmental stresses and maintain normal cell function. It also shows that the transmembrane potential did not reach the breakdown level as the membrane properties for the adhesion of the cell was not affected. If cells adhere and grow out, it is a quantitative measure for the viability of the cells [36]. The increased adhesion was mainly due to the presence of $CaCl_2$ in M2 and M3.

4 Conclusions

The use of low conductivity medium, n-DEP patterning and optimally designed microchip have collectively resulted in significant enhancement of cell viability and cell adhesion rate. Furthermore, for long-term cell culture, replacing the low conductive medium by native culture medium DMEM after patterning helped the cells maintain en-

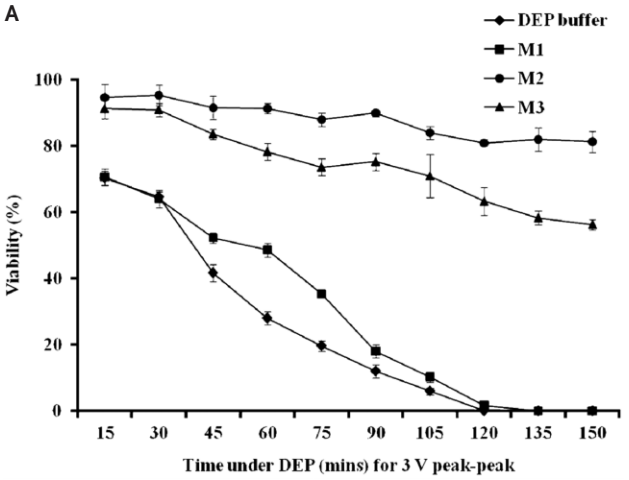

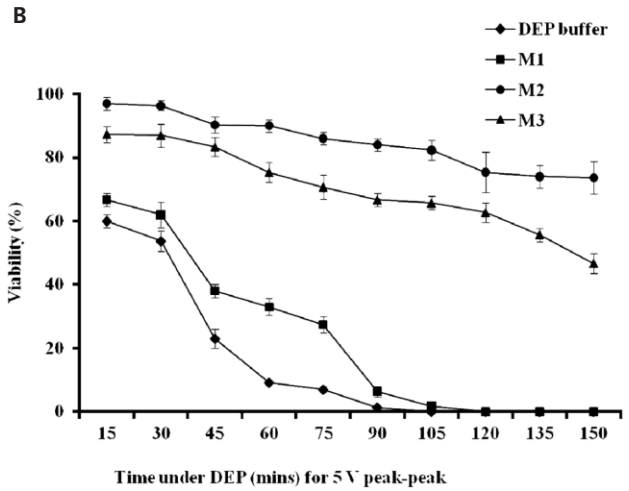

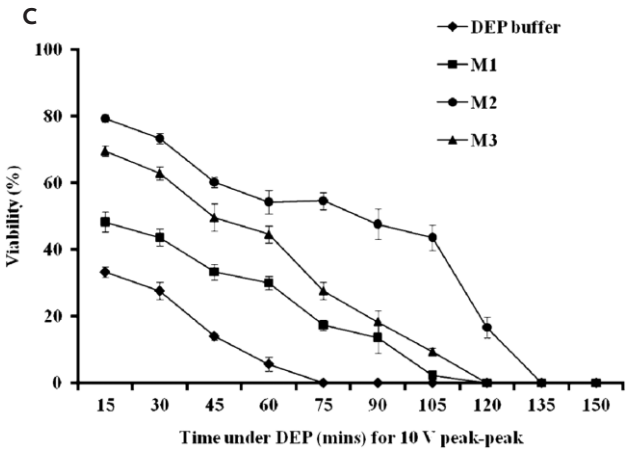

Figure 5. Viability of cells at varying AC electric voltage. (A) Viability of cells under 3 V peak-peak with minimum frequency required for different media to visualize high resolution patterning phenomena. (B) Viability of cells under 5 V peak-peak with minimum frequency required for different media to visualize high resolution patterning phenomena. (C)Viability of cells under 10 V peak-peak with minimum frequency required for different media to visualize high resolution patterning phenomena.

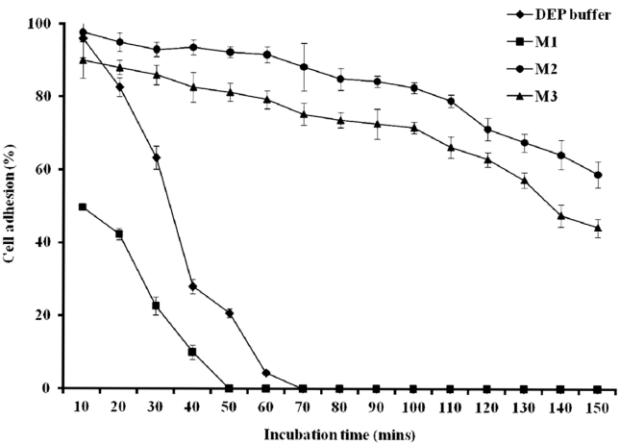

Figure 6. Adhesion rate of cells with incubation time in altered media.

hanced viability compared to buffer used previously. Among the three media assessed, M2 is the most appropriate for DEP manipulation. Using this medium, high resolution liver cells patterning can be achieved with less impact on viability and cell growth.

This research was financially supported by National Science Council through grant NSC 98-2120-M-007-003. The authors thank Prof. Hsing-Wen Sung and Mr. Kiran Sonje for help with osmolarity measurements and fruitful discussion. The formulated media were prepared with the help from Prof. Chin Yu and Dr.Sepuru Krishnamohan. The authors thank the Semiconductor Research Center and National Nano Device Laboratory for the access of microfabrication facility.

The authors have declared no conflict of interest.

5 References

[1] Pohl, H. A., The motion of precipitation of suspensoids in divergent electric Fields. *J. Appl. Phys.* 1951, *22*, 869–871.

[2] Hughes, M. P., *Nanoelectromechanics in Engineering and Biology*. CRC Press, Boca Raton 2002.

[3] Wang, X. B., Huang, Y., Burt, J. P. H., Selective dielectrophoretic confinement of bioparticles in potential energy wells. *J. Appl. Phys.* 1993, *26*, 1278–1285.

[4] Markx, G. H., Huang, Y., Zhou, X.-F., Dielectrophoretic characterization and separation of micro-organisms. *Microbiology* 1994, *140*, 585–591.

[5] Masuda, S., Washizu, M., Nanba, T., Novel method of cell fusion in field constriction area in fluid integrated circuit. *IEEE Trans. Ind. Appl*. 1989, *25*, 732–737.

[6] Washizu, M., Nanba, T., Masuda, S., Handling biological cells using a fluid integrated circuit. *IEEE Trans. Ind. Appl.* 1990, *26*, 352–356.

[7] Gimsa, J., Marszalek, P., Loewe, U., Tsong, T. Y., Dielectrophoresis and electrorotation of neurospora slime and murine myeloma cells. *Biophys. J*. 1991, *60*,749–760.
[8] Schnelle, T., Hagedorn, R., Fuhr, G., Fiedler, S. *et al*., Three-dimensional electric field traps for manipulation of cells-calculation and experimental verification. *Biochim. Biophys. Acta* 1993, *1157*, 127–140.
[9] Pavlin, M., Kanduser, M., Rebersek, M., Pucihar, G. *et al.,* Effect of cell electroporation on the conductivity of a cell suspension. *Biophys. J.* 2005, *88*, 4378–439.
[10] Glasser, H., Fuhr, G., Cultivation of cells under strong AC-electric field — Differentiation between heating an transmembrane potential effects. *Bioelectrochem. Bioenerg.* 1998, *47*, 301–310.
[11] Fuhr, G., Glasser, H., Muller, T., Schnelle, T., Cell manipulation and cultivation under a. c electric field influence in highly conductive culture media. *Biochim. Biophys. Acta* 1994, *1201*, 353–360.
[12] Zimmermann, U., Friedrich, U., Mussauer, H., Gessner, P. *et al*., Electromanipulation of mammalian cells: fundamentals and application. *IEEE Trans. Plasma Sci.* 2000, *28*, 72–82.
[13] Knox, J. H., McCormack, K. A., Temperature effects in capillary electrophoresis, some theoretical calculations and predictions. *Chromatographia* 1994, *38*, 215–221.
[14] Grushka, E., McCormick, R. M., Kirkland, J. J., Effect of temperature gradients on the efficiency of capillary zone electrophoresis separations. *Anal. Chem*. 1989, *61*, 241–246.
[15] Jones, A. E., Grushka, E., Nature of temperature gradient in capillary zone electrophoresis. *J. Chromatogr.* 1989, *466*, 219–225.
[16] Tang, G. Y., Yang, C., Chai, J. C., Gong, H. Q., Joule heating effect on electroosmotic flow and mass species transport in a microcapillary. *Int. J. Heat Mass Trans*. 2004, *47*, 215–227.
[17] Ho, C. T., Lin, R. Z., Chang, W. Y., Chang, H. Y. *et al*., Rapid heterogeneous liver-cell on-chip patterning via the enhanced field-induced dielectrophoresis traps. *Lab Chip* 2006, *6*, 724–734.
[18] Lin, R. Z., Ho, C. T., Liu, C. H., and Chang, H. Y., Dielectrophoresis based-cell patterning for tissue engineering. *Biotechnol. J.* 2006, *1*, 949–957.
[19] Fuhr, G., Voigt, A., Miiller, T., Wagner, B. *et al*., Electric-field-mediated inhibition of cell and microparticle adhesion: A new way to create bio- repellent surfaces. *Sensors Actuators B* 1995, *26–27*, 468–470.
[20] Ma, R., Han, C., Sun, Z., Huang, G. *et al*., A low conductivity culture medium suitable for the evaluation of sperm motility. *Abstracts of the Seventh International Conference on Photonics and Imaging in Biology and Medicine*, 2009, *7280*, 72800H 1–7.
[21] Bouaziz, A., Richert, A., Caprini, A., Morphological aspects of endothelial cells cultured in absence of foetal calf under controlled electrical charges applied to support. *Biomaterials* 1996, *17*, 2281–2287.
[22] Ho, C. T., Lin, R. Z., Chang, H. Y., Liu, C. H., Micromachined T-switches for cell sorting applications. *Lab Chip* 2005, *5,* 1248–1258.
[23] Gismari, M. S., Fernando, R. X. S., Maria F. C. P.,Adherence to HeLa cells, typing by killer toxins and susceptibility to antifungal agents of *Candida dubliniensis* strains. *Braz. Oral Res.* 2007, *21*, 1.
[24] Gard, A. L., Burrell, M. R., Pfeiffer, S. E., Rudge, J. S. *et al*., Astroglial control of oligodendrocyte survival mediated by PDGF and Leukemia Inhibitory Factor-like protein. *Development* 1995, *121*, 2187–2197.
[25] Thomas, R. S., Morgan, H., Green, N. G., Negative DEP traps for single cell immobilisation. *Lab Chip* 2009, *9*, 1534–1540.
[26] Cheung, W. Y., Calmodulin plays a pivotal role in cellular regulation. *Science* 1980, *202*, 19–27.
[27] Friedmann, N. K., Feng, L., The role of intracellular Ca^{2+} in the regulation of gluconeogenesis. *Metabolism* 1996, *42*, 389–403.
[28] Heizmann, C. W., Hunziker, W., Intracellular calcium-binding proteins: More sites than in sights. *Trends Biochem. Sci.* 1991, *16*, 98–103.
[29] Pucihar, G., Kotnik, T., Kanduser, M., Miklavcic, D., The influence of medium conductivity on electropermeabilization and survival of cells *in vitro*. *Bioelectrochemistry* 2001, *54*, 107–115.
[30] Gallant, N. D., Michael, K. E., García**,** A. J., Cell adhesion strengthening: Contributions of adhesive area, integrin binding and focal adhesion assembly. *Mol. Biol. Cell* 2005, *16*, 4329–4340.
[31] Garcia, A. J., Ducheyne, P., Boettiger, D., Quantification of cell adhesion using a spinning disc device and application to surface-reactive material. *Biomaterials* 1997, *18*, 1091–1098.
[32] Goldstein, A. S., DiMilla, P. A., Comparison of converging and flow for measuring cell diverging radial adhesion. *Bioeng. Food Nat. Products* 1998, *44*, 465–473.
[33] Christ, K. V., Williamson, K. B., Masters K. S., Turner, K. T., Measurement of single-cell adhesion strength using a microfluidic assay. *Biomed. Microdevices* 2010, *12*, 443–455.
[34] Engler, A. J., Chan, M., Boettiger, D., Schwarzbauer, J. E., A novel mode of cell detachment from fibrillar fibronectin matrix under shear. *J. Cell Sci.* 2009, *122*, 1647–1653.
[35] Humphries, M. J., Cell adhesion assays. *Mol. Biotechnol*. 2001, *18*, 57–61.
[36] Heida, T., Vulto, P., Rutten, W. L. C., Marani, E., Viability of dielectrophoretically trapped neural cortical cells in culture. *J. Neurosci. Methods* 2001, *110*, 37–44.

